The zebrafish Iroquois gene *iro7* positions the r4/r5 boundary and controls neurogenesis in the rostral hindbrain

Virginie Lecaudey[1,2], Isabelle Anselme[1,2], Frédéric Rosa[1] and Sylvie Schneider-Maunoury[1,2,*]

[1]Unité de Biologie Moléculaire du Développement, Unité INSERM 368, Ecole Normale Supérieure, 46, rue d'Ulm, 75005 Paris, France
[2]Unité de Biologie du Développement, UMR CNRS 7622, Université Pierre et Marie Curie, 9 quai Saint Bernard, 75005 Paris, France
*Author for correspondence (e-mail: maunoury@wotan.ens.fr)

Accepted 24 March 2004

Development 131, 3121-3131
Published by The Company of Biologists 2004
doi:10.1242/dev.01190

Summary

Early brain regionalisation involves the activation of genes coding for transcription factors in distinct domains of the neural plate. The limits of these domains often prefigure morphological boundaries. In the hindbrain, anteroposterior patterning depends on a segmentation process that leads to the formation of seven bulges called rhombomeres (r). The molecular cues involved in the early subdivision of the hindbrain and in rhombomere formation are not well understood. We show that *iro7*, a zebrafish gene coding for a transcription factor of the Iroquois family, is expressed at the end of gastrulation in the future midbrain and hindbrain territories up to the prospective r4/r5 boundary. This territory is strictly complementary to the expression domain of another homeobox gene, *vhnf1*, in the caudal neural plate. We demonstrate that Iro7 represses *vhnf1* expression anterior to their common border and that, conversely, vHnf1 represses *iro7* expression caudal to it. This suggests that the r4/r5 boundary is positioned by mutual repression between these two transcription factors. In addition, *iro7* is involved in the specification of primary neurons in the rostral hindbrain. In particular, it is essential for the formation of the Mauthner neurons in r4. We propose that *iro7* has a dual function in the hindbrain of the zebrafish embryo: it is required for the proper positioning of the prospective r4/r5 boundary and it promotes neurogenesis in the anterior hindbrain.

Key words: Iroquois, *iro7*, *vhnf1* (*tcf2*), Hindbrain, Boundary, Rhombomere, Neurogenesis

Introduction

Anteroposterior (AP) patterning of the vertebrate brain begins during gastrulation in the newly formed neural plate. Signals from adjacent tissues activate the expression of transcription factor genes in distinct domains of the neural plate (reviewed by Lumsden and Krumlauf, 1996). The limits of these expression territories often prefigure morphological boundaries and may be the site of formation of secondary signalling centres that act to organise adjacent tissues (Larsen et al., 2001; Kobayashi et al., 2002) (reviewed by Lumsden and Krumlauf, 1996; Wurst and Bally-Cuif, 2001).

In the hindbrain, AP patterning involves a segmentation process that leads to the formation of seven transient bulges called rhombomeres (r) and establishes the reiterated organisation of cranial nerves. The rhombomeres are segmental units for neuronal differentiation and gene expression, and constitute cellular compartments (for reviews, see Lumsden and Krumlauf, 1996; Schneider-Maunoury et al., 1998; Moens and Prince, 2002). Hindbrain segmentation is also crucial for patterning and migration of the neural crest, thereby influencing face and neck morphogenesis (for a review, see Trainor and Krumlauf, 2000), and for the formation of the otic vesicle, the prospective inner ear (for a review, see Torres and Giraldez, 1998).

Rhombomere formation proceeds by successive steps. Before segmentation is morphologically conspicuous, regulatory genes such as the Hox genes *hoxb1b* (*Hoxa1*) and *hoxb1a* (*Hoxb1*), *valentino* (*mafb* – Zebrafish Information Network; the zebrafish orthologue of *Mafb*), a gene coding for a bZIP transcription factor, and *krx20* (*egr2b* – Zebrafish Information Network; *Egr2*), a gene coding for a zinc-finger transcription factor, are activated in the hindbrain, in distinct territories but with undefined limits (Wilkinson et al., 1989; Murphy and Hill, 1991; Cordes and Barsh, 1994) (for reviews, see Schneider-Maunoury et al., 1998; Moens and Prince, 2002). These transcription factors are involved both in the formation of different rhombomeres or groups of rhombomeres, and in the specification of their identity (Giudicelli et al., 2001; McClintock et al., 2001; Voiculescu et al., 2001; McClintock et al., 2002; Giudicelli et al., 2003) (reviewed by Morrison, 1998; Schneider-Maunoury et al., 1998). In a second step, the limits of gene expression sharpen and later correspond to morphologically conspicuous rhombomere boundaries (Irving et al., 1996; Moens and Prince, 2002). Boundary formation is triggered by cell segregation at the interfaces between adjacent pre-rhombomeric territories (Guthrie and Lumsden, 1991; Guthrie et al., 1993; Wizenmann and Lumsden, 1997). This cell-sorting mechanism is mediated by Eph/ephrin interactions (Xu et al., 1995; Xu et al., 1999). Finally, the establishment of a specific

pattern of gene expression, including Hox genes, in each rhombomere specifies positional identity along the AP axis and the fate of neuronal derivatives (Bell et al., 1999; Jungbluth et al., 1999) (reviewed by Rijli et al., 1998; Schneider-Maunoury et al., 1998). Inter-rhombomeric signalling is also involved in rhombomere specification, and in this respect r4 plays an important role in adjacent rhombomeres (Graham and Lumsden, 1996; Helmbacher et al., 1998; Marin and Charnay, 2000; Maves et al., 2002; Walshe et al., 2002).

The mechanisms that lead to the activation of regulatory genes such as *krx20* and *val* at precise positions along the AP axis and thereby to the formation of pre-rhombomeric territories during gastrulation are not well understood. In the posterior hindbrain, the expression of the homeobox gene *vhnf1* (*tcf2* – Zebrafish Information Network) is activated at the end of gastrulation, with a rostral limit that has been shown to lie within prospective r5 (Sun and Hopkins, 2001; Wiellette and Sive, 2003). *val* and *krx20* are activated at the beginning of somitogenesis, in prospective r5 and r6, and r3 and r5, respectively (Wilkinson et al., 1989; Cordes and Barsh, 1994). Recent studies have shown that, in zebrafish embryos, the activation of *val* in r5 and r6 and of *krx20* in r5 depends both on *vhnf1* and on FGF3/8 signalling from r4 (Sun and Hopkins, 2001; Maves et al., 2002; Walshe et al., 2002; Wiellette and Sive, 2003). However, the mechanisms involved in the establishment of the *vhnf1* expression domain, and in particular in the positioning of its anterior limit, are not known.

We have investigated the function of a zebrafish gene of the Iroquois (Iro) family, *iro7*. Iro genes code for homeodomain transcription factors of the TALE (three amino-acid loop extension) superfamily (Burglin, 1997). They are characterised by a highly conserved, 12 amino acid long domain called the Irobox (Cavodeassi et al., 2001). Iro genes were first described in *Drosophila*, where they perform essential functions in the patterning of the eye/antenna and wing imaginal discs (for reviews, see Cavodeassi et al., 2001; Gomez-Skarmeta and Modolell, 2002). Vertebrate Iro genes are involved in various embryonic patterning processes, such as heart, ectoderm and neural tube regionalisation (for reviews, see Cavodeassi et al., 2001; Gomez-Skarmeta and Modolell, 2002). They have also been shown to participate in the activation of proneural gene expression, both in *Drosophila* and vertebrates (Gomez-Skarmeta et al., 1996; Gomez-Skarmeta et al., 1998; Itoh et al., 2002).

iro7 is a divergent member of the Iro family. Its closest relatives are the members of the *irx1/irx3* paralogous group, suggesting that *iro7* is an orthologue of these genes that has diverged after duplication of the teleost genome (Lecaudey et al., 2001; Itoh et al., 2002). *iro7* shows an AP regionally restricted expression in the neural plate as early as 70% epiboly. At this stage, it is expressed in a large bilateral stripe, covering the neural plate and the future neural crest and placodal regions, and encompassing the prospective midbrain and hindbrain territories along the AP axis (Lecaudey et al., 2001; Itoh et al., 2002). Another zebrafish Iro gene, *iro1*, shows a similar expression pattern at the same stage, but its caudal limit is anterior to that of *iro7* (Itoh et al., 2002). *iro7* is necessary for the determination of neurons of the trigeminal placode, and *iro1* and *iro7* play partially redundant roles in the formation of the midbrain-hindbrain boundary (Itoh et al., 2002).

In this paper, we study the formation of the prospective r4/r5 boundary at the end of gastrulation. We show that the position of this boundary is set up by mutual repression between two transcription factors, Iro7 and vHnf1. In addition, *iro7* is required for neurogenesis in the rostral hindbrain. Thus, *iro7* is involved in two different aspects of the specification of hindbrain neuronal derivatives: AP patterning and neurogenesis.

Materials and methods

Zebrafish lines and maintenance

Zebrafish (*Danio rerio*) were raised and staged as previously described (Westerfield, 1994; Kimmel et al., 1995). The *vhnf1*^{hi2169} mutant (Sun and Hopkins, 2001) and the Isl1-GFP transgenic (Higashijima et al., 2000) lines were described previously.

Constructs

A cDNA encoding full-length *vhnf1* was cloned by RT-PCR from total RNA extracted from six- to eight-somite stage embryos. *iro7* and *vhnf1* cDNAs encoding full-length proteins were subcloned into the CS2+ vector (Rupp et al., 1994). The *iro7myc* expression vector was made by cloning *iro7* cDNA in the CS2+MT vector (Rupp et al., 1994). An inducible form of Iro7 was constructed by fusing the ligand binding domain of the human glucocorticoid receptor (hGR) (from pCS2mcs-hGR, a gift from U. Strähle and P. Blader), to the C-terminal end of Iro7. A mutant form of *vhnf1*, *vhnf1*^{Q139E}, was made by introducing a point mutation in the POU domain using the ExSite PCR-Based Site-Directed Mutagenesis Kit (Stratagene). Δ*N-iro7* (a gift from A. Chitnis) codes for a modified Iro7 protein missing the first nine amino acids, thus preventing its hybridisation with Moz7 (Itoh et al., 2002).

RNA and morpholino injection

Capped RNAs were transcribed with SP6 RNA polymerase using the mMessage mMachine Kit (Ambion). An antisense morpholino (Gene-Tools, Inc., Oregon, USA) was designed to target *iro7* (Moz7): 5′ GGCATCCTTACTCCCTGAGCTCTGG 3′, as well as a control morpholino (Moz7m): 5′ GGgATCgTTAgTCCgTGAcCTCaGG 3′, containing six mismatches. Morpholinos were injected at a concentration of 1 mM. In some RNA injections, *nls-lacZ* (75 ng/μl) or *GFP* (100 ng/μl) RNAs were added as lineage tracers. The translocation of the Iro7hGR protein into the nucleus was induced by transferring embryos into medium containing 10 μM Dexamethasone (Sigma D-4902) at 40% epiboly.

Whole mount in situ hybridisation and immunohistochemistry

In situ hybridisation and immunohistochemistry were performed as previously described (Hauptmann and Gerster, 1994). *iro7* (*Hin*dIII, T7), *ngn1* (*neurog1* – Zebrafish Information Network; *Eco*RI, T7), *wnt1* (*Eco*RI, Sp6) (gifts from A. Chitnis), *six3* (*Eco*RI, T3) and *vhnf1* (*Not*I, T7) (gifts from B. Thisse and C. Thisse), *hoxb1a*, *hoxa2* and *hoxb3* (Prince et al., 1998), *krox20* (Oxtoby and Jowett, 1993), *val* (Moens et al., 1998), *fgf3* (Kudoh et al., 2001), *fgf8* (Furthauer et al., 1997), and *pax2.1* (*pax2a* – Zebrafish Information Network) (Krauss et al., 1991) DNAs were used as templates for making RNA probes. For sectioning, embryos were embedded in resin (JB4, Polysciences). For immunohistochemistry, the following antibodies were used: mouse anti-neurofilament 3A10 (DSHB) (Hatta, 1992) and RMO44 (Zymed 13-0500) (Popperl et al., 2000) antibodies, mouse Islet 39.4D5 (DSHB) (Ericson et al., 1992), rabbit anti-β-galactosidase (Cappel 55976), rabbit anti-GFP (Molecular Probes A11122) and rabbit anti-Myc epitope (Upstate Biotechnology 06-549).

In vitro translation

Capped *iro7* RNA (20 ng/μl) was translated in vitro in the presence

of increasing concentrations of Moz7 or Moz7m (0.4 μM to 80 μM) using [^{35}S] methionine in a Rabbit reticulocyte lysate (Promega).

Statistical analyses

In Fig. 4, '*vhnf1* expression domain AP length' corresponds to the distance between the anterior and posterior borders of the *vhnf1* expression domain, including the most anterior domain of weaker expression. *P* is the probability associated with Student's *t*-test. The error bars correspond to the standard deviation.

Results

The caudal limit of the *iro7* expression territory corresponds to the prospective r4/r5 boundary

In previous work, we showed that *iro7* is expressed from 70% epiboly onward in a large bilateral stripe in the neural plate, corresponding to the future midbrain and hindbrain, and that at early somite stages its caudal limit is located in the r4/r5 region (Lecaudey et al., 2001). In order to determine more accurately the position of the caudal limit of *iro7* expression domain and its relations to pre-rhombomeric territories, we performed double in situ hybridisation with probes for *iro7*, *krx20*, *val*, *hoxb3* and *vhnf1*. *vhnf1* is expressed in the caudal neural plate with a rostral limit that has been proposed to lie within r5 at early somite (s) stages (Sun and Hopkins, 2001; Wiellette and Sive, 2003). *val* is expressed from the tailbud stage onward in prospective r5 and r6 (Moens et al., 1998). *krx20* is activated at the tailbud stage in prospective r3 and at the 1 s stage in prospective r5 (Oxtoby and Jowett, 1993). *hoxb3* is activated at the 1-2 s stage in the neural plate posterior to r5 and at the 3-4 s stage its expression overlaps r5 (Prince et al., 1998). We found that *vhnf1* expression was activated in the caudal neural plate at 70% epiboly. Up to 90% epiboly, its rostral limit remained slightly caudal to the caudal limit of *iro7* expression (Fig. 1A). From the 95% epiboly to the 2 s stages, the rostral limit of *vhnf1* expression abutted the caudal limit of *iro7* expression (Fig. 1B-E). The caudal limit of *iro7* expression also corresponded to the rostral limit of *val* expression from the tailbud stage onwards (Fig. 1F,G) and of *hoxb3* from the 3-4 s stage onwards (Fig. 1H). At the 1 s stage, *iro7* was expressed in prospective r3 and r4 (Fig. 1I). At this stage, the caudal *krx20* expression stripe (future r5) appeared just caudal to the *iro7* expression limit (arrowheads in Fig. 1I,J) and within the *vhnf1* expression territory (arrowheads in Fig. 1M,N). From the 3 s stage, as *krx20* expression expanded in r5, *vhnf1* was downregulated in this rhombomere (Fig. 1O) and then in r6 (Fig. 1P). While *vhnf1* retracted posteriorly, *iro7* expression became restricted to r4 (Fig. 1K,L). Therefore, our data show that, between 95% epiboly and 2 s, the *iro7* and *vhnf1* expression territories are complementary to each other, and that their common limit of expression prefigures the r4/r5 boundary (summarised in Fig. 1Q).

iro7 loss of function results in a reduction in the AP extent of the midbrain and anterior hindbrain

To investigate the function of *iro7* in the hindbrain, we used a morpholino antisense oligonucleotide to inhibit mRNA translation (Nasevicius and Ekker, 2000). We designed a morpholino encompassing the initiation codon of *iro7* mRNA (Moz7) and a derived control morpholino containing mutations at six different positions (Moz7m) to check for specificity. Moz7 was able to inhibit the translation of *iro7* capped RNA in an in vitro translation assay in a concentration-dependent manner. Translation was totally abolished in the presence of 8 μM Moz7, while it was not affected by 80 μM Moz7m (Fig. 2A). Injection of Moz7 in zebrafish embryos at the one- to four-cell stage led to defects in brain morphology at 30 hours post fertilisation (hpf): the anteroposterior extent of the midbrain and hindbrain was reduced, and the isthmus was often malformed (Fig. 2B) when compared with controls (Fig. 2C). The otic vesicles were also reduced in size along the AP axis, taking up a round shape (Fig. 2B,C). In the course of our experiments, we never observed any difference between mock-injected, Moz7m injected and uninjected embryos, so they will hereafter be referred to as 'control embryos'.

As *iro7* is initially expressed in a large stripe covering the midbrain and anterior hindbrain, we investigated whether these territories were affected in embryos lacking *iro7* function, using molecular landmarks. During somitogenesis, *pax2.1* is expressed in the otic vesicle, in the optic stalk and at the MHB (Krauss et al., 1991), and *wnt1* is expressed at the MHB, in the

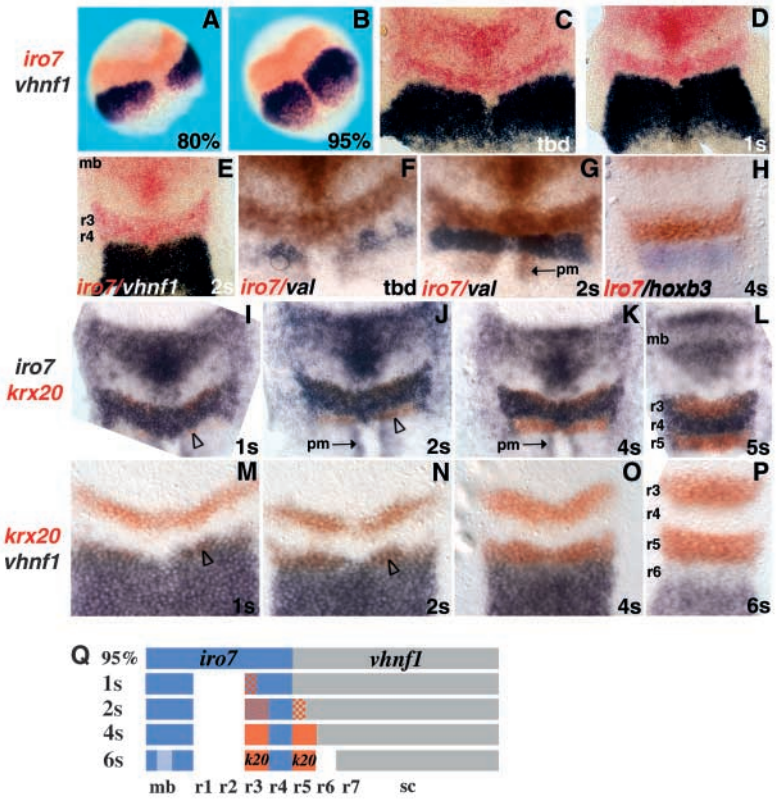

Fig. 1. *iro7* is expressed in a restricted domain of the neural plate with a posterior border at the prospective r4/r5 boundary. (A-P) Embryos stained by double in situ hybridisation with the indicated probes (colour coded). Anterior is towards the top, stages are indicated at the bottom right-hand corner of each picture. (A,B) Whole mounts; (C-P) flat mounts. The arrowheads in I,J,M,N indicate *krx20*-expressing cells in prospective r5. The arrows in G,J,K indicate a mesodermal domain of *iro7* expression (pm for paraxial mesoderm). (Q) Summary of expression data, anterior is towards the left. mb, midbrain; sc, spinal cord.

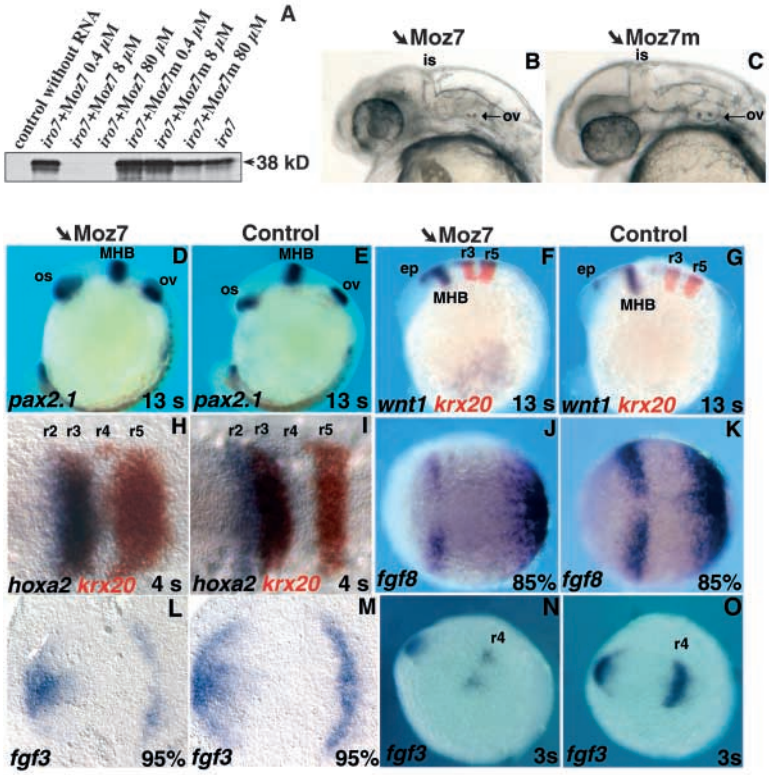

Fig. 2. Blocking *iro7* translation with Moz7 leads to a reduction of the midbrain and anterior hindbrain. (A) Autoradiography showing radiolabelled in vitro translation products of the *iro7* capped RNA in the presence of increasing concentrations of Moz7 or Moz7m (0.4 μM to 80 μM). (B,C) Lateral view of live embryos at 30 hpf injected with Moz7 (B) or Moz7m (C), anterior is towards the left. (D-O) Embryos stained by in situ hybridisation with the indicated probes (colour coded). Anterior is towards the left, stages are indicated at the bottom right-hand corner of each picture. (B-G,J,K,N,O) Whole mounts; (H,I,L,M) flat-mounts. is, isthmus; ov, otic vesicle; os, optic stalk; MHB, midbrain-hindbrain boundary; ep, epiphysis.

dorsal neural tube and in the epiphysis (Krauss et al., 1992). In Moz7-injected embryos stained for *pax2.1* at the 13 s stage, the domains located between the otic placode and the MHB, and between the MHB and the optic stalk, were shorter along the AP axis (Fig. 2D) when compared with control embryos (Fig. 2E). Similarly, double *wnt1/krx20* staining showed that the domains between the MHB and r3, and between the MHB and the epiphysis, were reduced along the AP axis in Moz7-injected embryos (Fig. 2F,G). These data showed that in the absence of *iro7* function, a large domain comprising the midbrain and the anterior hindbrain was reduced in size.

In order to better characterise the anterior hindbrain defects, we analysed the expression of *hoxa2*, *fgf8* and *fgf3* at the end of gastrulation and/or beginning of somitogenesis. *hoxa2* is expressed in future r2 and r3 from the 2 s stage onwards (Prince et al., 1998). *fgf8* is expressed in the anterior hindbrain, in a large domain that resolves at the 1 s stage into domains at the MHB/r1, ventral r2 and r4 (Maves et al., 2002; Walshe et al., 2002). *fgf3* is activated in a transverse stripe in the hindbrain at 90% epiboly, and is expressed at a high level in r4 at early somite stages (Maves et al., 2002; Walshe et al., 2002). In Moz7-injected embryos, the expression domains of *hoxa2* in r2-r3 (Fig. 2H), *fgf8* in MHB-r4 (Fig. 2J) and *fgf3* in r4 (Fig. 2L,N) were reduced in intensity and AP extent when compared with control embryos (Fig. 2I,K,M,O), but none of them was totally absent.

iro7 loss of function results in anterior expansion of r5 at the expense of r4

We then investigated the phenotypes caused by the loss of iro7 function at its posterior expression border. In Moz7 injected embryos stained for *krx20*, r3 and r5 were differently affected. Whereas the r3 stripe was occasionally reduced, consistent with the reduction in size of the anterior hindbrain, the r5 stripe was always expanded (Fig. 2F-I; Fig 3A-D). In addition, the gap between the r3 and r5 stripes was strongly reduced, suggesting that the r5 domain of *krx20* expression [*krx20* (r5)] expanded anteriorly into r4. This phenotype was already detectable at the onset of *krx20* expression: whereas the r3 stripe was slightly thinner, the r5 stripe was stronger and cells expressing *krx20* were present in r4 (Fig. 3E-H). To evaluate more accurately the anterior expansion of r5 and the reduction of r4, we measured the AP length of r4 and r5 on a batch of flat-mounted 6 s stage embryos. The anterior expansion of the *krx20* (r5) stripe was detected in 100% of the injected embryos (n=29), when compared to control embryos (n=11), and covered about half of r4 (mean increase of *krx20* (r5) AP length: 40%, P<0.01). Isolated *krx20*-expressing cells were often present in r4 (Fig. 3C,G). These cells were mostly localised medially in the neural plate and then ventrally in the neural tube, often forming a bridge of *krx20*-expressing cells between r3 and r5. To check if the expansion of *krx20* (r5) expression was specifically due to the inhibition of *iro7* translation by Moz7, we tried to rescue this phenotype by injecting Δ*N-iro7*, a modified form of *iro7* that does not hybridise with the morpholino. The injection of Δ*N-iro7* together with the morpholino led to a recovery of the size of r5, which was not statistically different from that of control embryos [mean increase 4.7% (n=19) compared with 40% (n=29) for Moz7-injected embryos]. The number of isolated *krx20*-expressing cells in r4 was also significantly reduced in rescued embryos (data not shown).

val is expressed from bud stage onwards in r5 and r6, and is necessary for the activation of *krx20* in r5 (Moens et al., 1998). Moz7 injection led to an expansion of the *val* expression domain (Fig. 3I,K), when compared with controls (Fig. 3J,L). Double *krx20/val* in situ hybridisation experiments showed that this expansion occurred anteriorly, was always limited to r4 and coincided with the expansion of the *krx20* expression domain (Fig. 3I,K). By contrast, the r6 domain of *val* expression did not seem affected (Fig. 3K). This confirmed that the expansion of r5 occurs anteriorly, at the expense of r4.

hoxb1a is activated at 90% epiboly in a broad domain with an anterior border at the r3/r4 boundary (Prince et al., 1998). Shortly after its activation, *hoxb1a* expression is upregulated in r4 and maintained at a high level in this rhombomere (McClintock et al., 2001) (Fig. 3N). In Moz7-injected

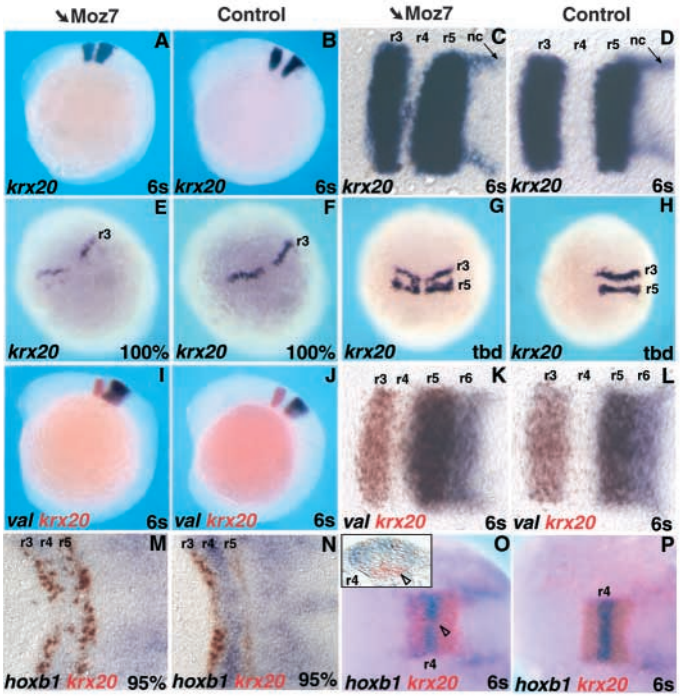

Fig. 3. Knocking-down *iro7* results in an anterior expansion of r5 at the expense of r4. (A-P) Whole-mount in situ hybridisation with the probes indicated (bottom left of each picture, colour coded) on embryos injected with Moz7 (A,C,E,G,I,K,M,O) or control embryos (B,D,F,H,J,L,N,P). Anterior is towards the left, except in E-H where anterior is towards the top. The inset in O presents a transverse section at the level of r4. The arrowheads indicate a group of cells expressing *krx20* ectopically in the ventral part of r4. (C,D,K,L,M,N) Dorsal views of flat-mounted embryos. Stages are indicated at the bottom right of each picture. nc, neural crest.

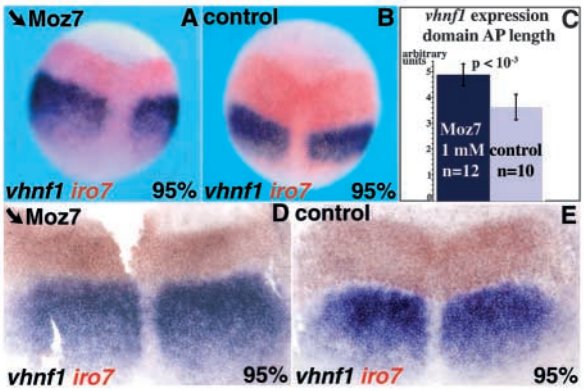

Fig. 4. Knocking-down *iro7* results in an anterior expansion of *vhnf1* expression. (A,B,D,E) Whole-mount in situ hybridisation with the probes indicated (bottom left, colour coded) on Moz7 injected (A,D) or control (B,E) embryos. All pictures are dorsal views of whole-mount (A,B) or flat-mounted (D,E) embryos, with anterior towards the top. (C) A mean increase of 34% (*t*-test; $P<0.001$) of the AP length of *vhnf1* expression domain in Moz7-injected embryos compared with control embryos.

embryos, *hoxb1a* expression was activated normally at 90% epiboly in the caudal neural plate (data not shown) but was not reinforced in r4 at the end of gastrulation, as it was in control embryos (Fig. 3M,N). Later, the AP extent of the r4 *hoxb1a* expression domain was reduced when compared with controls, and coincided with the gap between *krx20*-expressing cells in r3 and r5 (Fig. 3O,P). In this domain, cells lacking *hoxb1a* expression were frequently observed ventrally (Fig. 3O, inset in O). These gaps of *hoxb1a* expression coincided with the bridges of *krx20*-expressing cells in r4 (arrowheads in Fig. 3O).

In conclusion, the loss of *iro7* function leads to an anterior expansion of r5 at the expense of r4: the *krx20* (r5) and *val* expression domains are expanded anteriorly, and the *hoxb1a* expression domain in r4 is reduced.

iro7 loss-of-function results in an anterior shift of *vhnf1* rostral expression limit

Ectopic expression of *vhnf1* leads to ectopic activation of *val* and *krx20* in r4, and to a reduction of *hoxb1a* expression in this rhombomere (Sun and Hopkins, 2001; Wiellette and Sive, 2003), a phenotype very similar to that obtained after Moz7 injection. Therefore, we tested whether knocking-down *iro7* had any effect on *vhnf1* expression, by performing double in situ hybridisation experiments with probes for *vhnf1* and *iro7*. In Moz7-injected embryos at 95% epiboly to tailbud stages, the *vhnf1* expression territory was expanded anteriorly by about one-third, while the territory expressing *iro7* was reduced (Fig. 4A-E). We conclude from these experiments that *iro7* is necessary for the repression of *vhnf1* in the anterior hindbrain.

Ectopic expression of *iro7* results in a repression of *vhnf1*, *val* and *krx20* expression

As shown above, *iro7* is necessary for the repression of *vhnf1* and, probably as a consequence, of *val* and *krx20*. In order to determine whether *iro7* was sufficient to repress *vhnf1*, *val* and *krx20* in the caudal hindbrain, we performed *iro7* gain-of-function experiments. Injection of RNA coding for a Myc-tagged Iro7 protein (Iro7myc) led to frequent gastrulation defects (data not shown), hampering analysis of hindbrain patterning. Therefore, we also injected RNA coding for an inducible form of Iro7, Iro7hGR, which translocates into the nucleus upon dexamethasone (Dex) treatment, and treated the injected embryos with Dex at 40% epiboly. *GFP* RNA was co-injected as a tracer. In embryos injected with either *iro7myc* or *iro7hGR*, we observed a repression of *vhnf1* (Fig. 5A,B,D), *val* (Fig. 5F,H) and *krx20* (Fig. 5J,L,M). However, a high concentration of RNAs (40 ng/μl for *iro7myc* and 100 ng/μl for *iro7hGR*) was necessary to obtain these effects. Immunostaining with the anti-GFP or anti-Myc antibodies showed that the domain of repression of *vhnf1*, *val* and *krx20* always correlated with the injected regions, although not all injected cells showed a phenotype (Fig. 5A,D,H,L,M). In a batch of injected embryos, the proportion of embryos showing a domain of repression relative to the embryos expressing GFP or Myc in the region of interest was 22/53 for *vhnf1*, 14/16 for *val* and 11/15 for *krx20*. None of the *GFP*-injected control embryos showed repression of *vhnf1*, *val* or *krx20* expression (Fig. 5C,E,G,I,K,N). In addition, *krx20* expression was repressed specifically in r5, even though GFP staining was present in both r3 and r5 (Fig. 5L,M). Together, these results show that Iro7 is able to repress *vhnf1*, *val* and *krx20* expression. However, this repression is not fully penetrant,

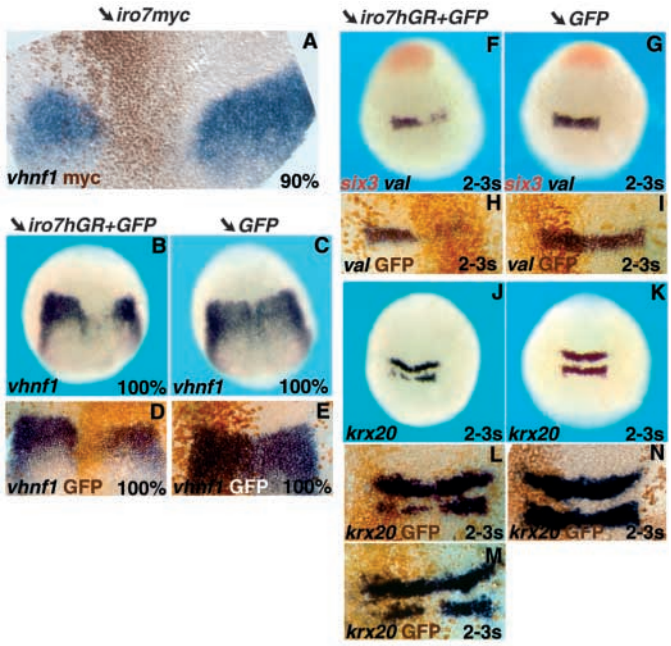

Fig. 5. Ectopic expression of *iro7* is sufficient to repress *vhnf1*, *val* and *krx20*. (A-N) Dorsal views of whole-mount (B,C,F,G,J,K) or flat-mounted (A,D,E,H,I,L,M,N) embryos analysed by in situ hybridisation and/or immunohistochemistry with the markers indicated (bottom left-hand corner of each picture, colour coded) on embryos injected with *iro7myc* (40 ng/μl) (A), *iro7hGR* (100 ng/μl) and *GFP* (B,D,F,H,J,L,M), or *GFP* alone (C,E,G,I,K,N). Anterior is towards the top.

suggesting that Iro7 requires co-factors that are either regionally restricted or present in limiting amounts.

vhnf1 represses *iro7* expression

As *vhnf1* and *iro7* expression domains are complementary at the end of gastrulation, *vhnf1* could also be involved in positioning the r4/r5 boundary by repressing *iro7* expression. To test this hypothesis, we analysed *iro7* expression in *vhnf1*^{hi2169} mutants, which carry a strong hypomorphic or null mutation in the *vhnf1* gene (Sun and Hopkins, 2001). Analysis of *krx20* expression allowed us to unambiguously identify homozygous mutants, as the *vhnf1* mutation leads to a loss of *krx20* expression in r5 (Sun and Hopkins, 2001). In these embryos, the caudal territory of *iro7* expression expanded posteriorly when compared with control siblings (Fig. 6A-E). These data showed that *vhnf1* is required for *iro7* repression in r5. As the caudal expansion was nevertheless limited to about one rhombomere length, other factors present in the caudal neural plate must also be able to repress *iro7* expression. Alternatively, *iro7* activation may itself be restricted to this region of the hindbrain. We also observed such a limited caudal expansion in *vhnf1*^{hi2169} homozygous embryos for *fgf8* (data not shown), whereas a wider caudal expansion was observed for *fgf3* (data not shown) and *hoxb1a* (Sun and Hopkins, 2001) (data not shown).

To further investigate the repressive activity of *vhnf1* on *iro7*, we tested whether *vhnf1* is sufficient to repress *iro7* anterior to the r4/r5 boundary. We expressed *vhnf1* ectopically by RNA injection. *Escherichia coli lacZ* RNA was co-injected as a lineage tracer. *vhnf1* ectopic expression resulted in a repression of *iro7* (Fig. 6F,G). All the cells that had downregulated *iro7* expressed β-galactosidase, suggesting that *vhnf1* represses *iro7* in a cell-autonomous manner (Fig. 6G). To check for the specificity of this repression, we injected RNA coding for a modified form of vHnf1 with a mutation within the POU domain (vHnf1^{Q139E}). An equivalent mutation in the human HNF1 protein abolishes its DNA-binding ability (S. Cereghini and C. Masdeu, unpublished). Injection of *vhnf1*^{Q139E} RNA had no effect on *iro7* expression (Fig. 6H). Thus, *vhnf1* is able to repress *iro7* expression. We conclude from these experiments that *vhnf1* is required for positioning the future r4-r5 boundary by repressing *iro7* expression in r5.

Knocking down *iro7* results in a loss of primary neurons in the anterior hindbrain

We sought to determine whether the patterning defects observed after Moz7 injection had any consequence on hindbrain neuronal derivatives. Two types of primary neurons are readily identifiable in the hindbrain of early zebrafish embryos and follow a segmental pattern: reticulospinal (RS) neurons and motoneurons (Metcalfe et al., 1986; Hanneman et al., 1988; Chandrasekhar et al., 1997). We analysed the pattern of RS neurons by immunostaining with the anti-neurofilament antibody RMO44 (Fig. 7A,B). This antibody identifies the hindbrain RS neurons with characteristic shapes and positions, such as Mauthner neurons in r4, and RoL2 neurons in r2 (arrowhead and arrow, respectively, in Fig. 7B) (Popperl et al., 2000). We found that r4-derived Mauthner neurons were always lost in Moz7-injected embryos (empty arrowhead in Fig. 7A), whereas r2-derived RoL2 neurons were in some cases also affected (empty arrow in Fig. 7A), although with a lower penetrance. We did not detect any modification in the pattern of RS neurons

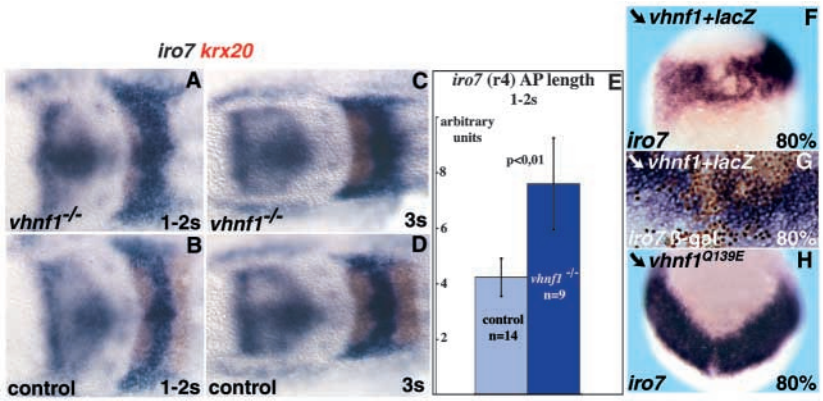

Fig. 6. *vhnf1* represses *iro7* expression. (A-D) Double in situ hybridisation with probes for *iro7* (blue) and *krx20* (red) on *vhnf1* homozygous (A,C) or control (B,D) embryos. (E) The statistical analysis of the posterior expansion of the *iro7* expression domain in *vhnf1* homozygous mutant embryos at 1-2 s. (F-H) In situ hybridisation with an *iro7* probe on embryos injected with *vhnf1* (20ng/μl) and *lacZ* (F,G) or with *vhnf1*^{Q139E} (25 ng/μl) (H) RNAs.
(G) Immunohistochemistry with an antibody directed against β-galactosidase.

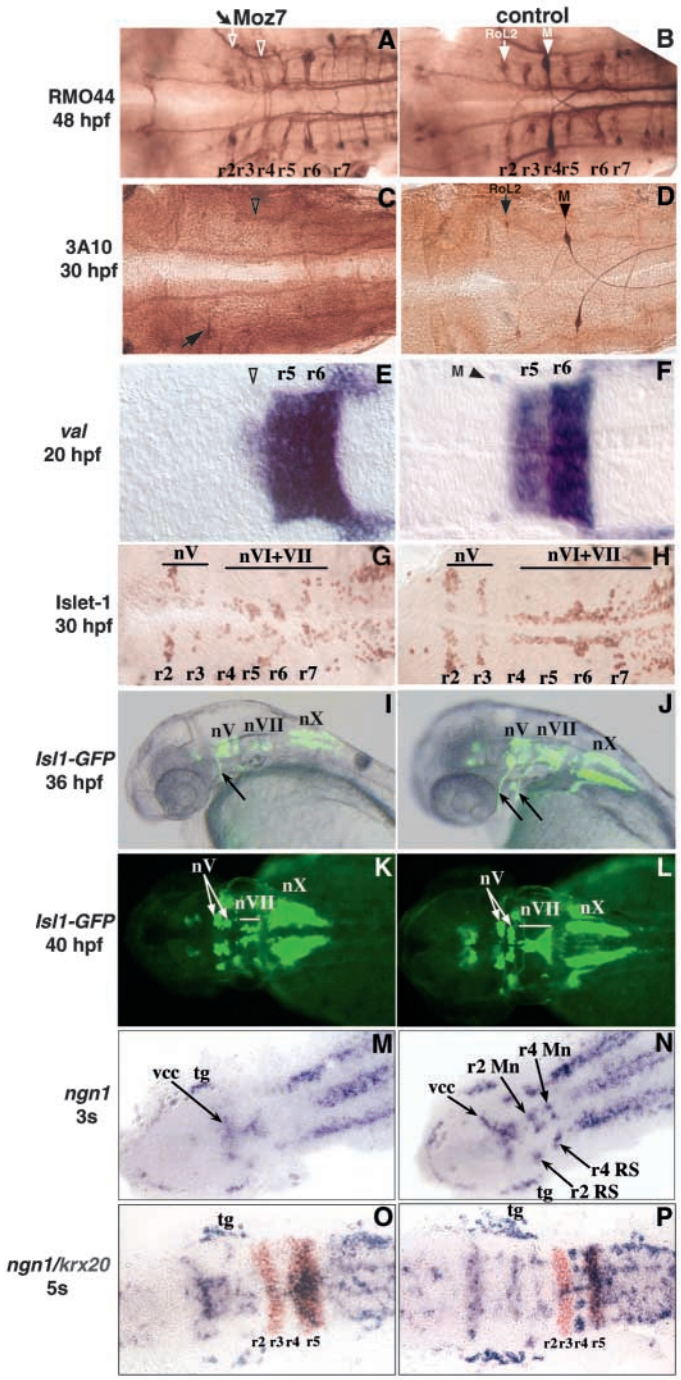

Fig. 7. Knocking-down *iro7* results in a reduction of neurogenesis in the anterior hindbrain. (A-D,G,H) Immunohistochemistry using anti-neurofilament RMO44 (A,B), 3A10 (C,D) or anti-Isl1 (G,H) antibodies on Moz7-injected (A,C,G) or control (B,D,H) embryos. (E,F) In situ hybridisation with a *val* probe on 20 hpf Moz7-injected (E) or control (F) embryos. (A-F) The r4-specific Mauthner neurons ('M', arrowhead in B,D,F) and the RoL2 neurons (arrows in B-D) are partially or totally lost after Moz7 injection (empty arrowheads and empty arrows in A,C,E). (I-L) Lateral views (I,J) or dorsal views (K,L) of live Isl1-GFP transgenic embryos injected with Moz7 (I,K) or uninjected (J,L). (G-L) nV, nVI, nVII and nX indicate the motor nuclei of the Vth, VIth, VIIth and Xth nerves, respectively. Arrows in I,J indicate the trigeminal (anterior) and facial (posterior) motor nerves. (M-P) Flat-mounted embryos analysed by in situ hybridisation with the probes indicated on the left (colour-coded) on Moz7-injected (M,O) or Moz7m-injected (N,P) embryos. Anterior is towards the left. Proneural clusters are indicated as follows: Mn, motoneurons; tg, trigeminal ganglion; RS, reticulospinal neurons; vcc, ventrocaudal cluster.

caudally to r4 (Fig. 7A,B). To confirm this phenotype, we used two earlier markers of the Mauthner neurons: the anti-neurofilament antibody 3A10, which stains strongly Mauthner neurons at 30 hpf (Furley et al., 1990) (Fig. 7D), and *val*, which is expressed in Mauthner neurons at 20 hpf in addition to r5, r6 and associated neural crest cells (Moens et al., 1998) (Fig. 7F). These two markers confirmed the total loss of Mauthner neurons in *iro7* morphants (empty arrowheads in Fig. 7C,E). In total, r4-derived Mauthner cells were lost in 94% of the Moz7-injected embryos (n=119).

The pattern of motoneurons was analysed using an antibody against the Isl1 protein (Fig. 7G,H) or by injecting Moz7 into Isl1-GFP transgenic embryos (Higashijima et al., 2000) (Fig. 7I-L). In zebrafish embryos, Vth (trigeminal) motoneurons originate in two discrete groups in r2 and r3 and migrate laterally in these two rhombomeres (Chandrasekhar et al., 1997). VIIth (facial) motoneurons originate in r4 and migrate caudally and then laterally to reach their final position in r6 and r7 (Chandrasekhar et al., 1997; Higashijima et al., 2000; McClintock et al., 2001). The motor axons of the Vth and VIIth nerves (arrows in Fig. 7J) leave the hindbrain at the level of r2 and r4 to innervate the first and second branchial arches, respectively. VIth (abducens) motoneurons are born in r5 and r6. In contrast to the Isl1 antibody, Isl1-GFP does not label abducens motoneurons (Higashijima et al., 2000). In Moz7-injected embryos, there was an overall reduction in the population of trigeminal and facial branchiomotor neurons (Fig. 7G,I,K) when compared with controls (Fig. 7H,J,L). The motoneurons of the facial nucleus, that are born in r4, were however more affected: the size of this nucleus was reduced by 60 to 80% (Fig. 7K,L). As these neurons migrate caudally to reach their final destination in r6 and r7, this resulted in an overall perturbation of the motoneuronal organisation in the r5-r7 region (Fig. 7, compare G,K with H,L). Motoneurons of the IXth and Xth nerves and spinal motoneurons were not affected (Fig. 7I,K and data not shown). Motor axons could always be detected in the trigeminal nerve in *iro7* morphants (arrow in Fig. 7I), whereas the facial motor nerve was missing in 75% of the Moz7-injected embryos (n=8) (Fig. 7I). Together these results showed that *iro7* is essential for the specification of primary neurons in the anterior hindbrain, and in particular for r4-derived neurons.

We wondered whether these defects in the pattern of primary neurons could be the result of a downregulation of proneural gene expression. Indeed, recent data showed that *iro7* is involved in the formation of the trigeminal ganglion and in the expression of the proneural gene *ngn1* in the trigeminal placode; moreover, *iro7* ectopic expression is able to activate *ngn1* expression ectopically (Itoh et al., 2002). Consistently, we found that Moz7 injection led to a reduction of *ngn1* expression in the anterior hindbrain region at the onset of somitogenesis (Fig. 7M-P). In r4, the proneural clusters that give rise to RS interneurons (dorsal clusters, r4 RS) and to

motoneurons (ventral clusters, r4 Mn) were absent after Moz7 injection (Fig. 7, compare M,O with N,P) (96% of the injected embryos, *n*=23).

In conclusion, the knockdown of *iro7* leads to an overall reduction in the number of primary neurons derived from the r2 to r4 region, with a more pronounced effect in r4. Moz7 injection also leads to a loss or strong downregulation of *ngn1* expression, strongly suggesting that the reduction of RS and motoneuronal populations is due to a function of *iro7* in the activation of proneural gene expression in the anterior hindbrain.

Discussion

In this paper, we investigated the function in hindbrain patterning of *iro7*, a gene coding for a homeodomain-containing transcription factor of the Iroquois family. We showed that the r4/r5 boundary forms at the interface between the expression territories of *iro7* rostrally and *vhnf1*, another homeobox gene, caudally. Gain and loss-of-function experiments demonstrated that these two transcription factors position the boundary by mutual repression. Finally, in addition to its role in early patterning of the hindbrain, *iro7* is required for neurogenesis in the r2 to r4 region.

iro7 is required to set up the position of the r4/r5 boundary

Although hindbrain segmentation has been extensively studied, the mechanisms underlying its early AP patterning and, in particular, those involved in the formation and positioning of early pre-rhombomeric territories and of their boundaries are still poorly understood. In zebrafish, the first boundaries to appear morphologically are the r3/r4 and the r4/r5 boundary (Maves et al., 2002). Until now, the posterior border of the domain expressing *hoxb1a* at a high level (prospective r4) was the first evidence of the future r4/r5 boundary. *iro7* is expressed from 70% epiboly in a transversal stripe in the neural plate (Lecaudey et al., 2001; Itoh et al., 2002) and we demonstrate in this paper that its posterior expression border corresponds to the future r4/r5 boundary. Thus, the posterior border of the *iro7* expression domain represents an early limit in the developing hindbrain at the position of the r4/r5 boundary, in a way similar to *hoxb1b* (*Hoxa1*), whose anterior expression border prefigures the r3/r4 boundary at mid-gastrulation (Murphy and Hill, 1991; Prince et al., 1998; McClintock et al., 2001). Slightly later, *vhnf1* expression is activated in the posterior neural plate and is required for the expression of *val* in r5 and r6 and of *krx20* in r5 (Sun and Hopkins, 2001). We show that *iro7* and *vhnf1* have strictly complementary expression domains between 95% epiboly and 2 s. Thereby, *vhnf1* is the earliest gene expressed in the caudal neural plate in a domain adjacent to that of *iro7* expression. Altogether, these results make *iro7* and *vhnf1* good candidates to set up the prospective r4/r5 boundary by mutual repression.

In this paper, we demonstrate that *vhnf1*, *val* and *krx20* (r5) expression territories are expanded anteriorly in *iro7* morphants, and that ectopic expression of *iro7* represses *vhnf1*, *val* and *krx20* expression in the posterior hindbrain. Thus, *iro7* is indeed required to set up the position of the r4/r5 boundary by repressing *vhnf1* expression anteriorly. In *iro7* ectopic expression experiments, the repression of *vhnf1*, *val* and *krx20* expression by *iro7* is not fully penetrant, suggesting that Iro7 requires co-factors that are either regionally restricted or present in limiting amount. Consistent with this hypothesis, Iroquois proteins belong to the TALE superfamily of transcription factors and other members of this group, such as Meis and Pbx proteins, form multimeric complexes (Ferretti et al., 2000; Choe et al., 2002).

We propose that the prospective r4/r5 boundary is set up at the end of gastrulation/beginning of somitogenesis by mutual repression between two homeodomain transcription factors, Iro7 and vHnf1. However, the expression domains of these two genes are only transiently complementary, between the 95% epiboly and 2 s stages. Therefore, the maintenance of the boundary may later involve mutual repression between Iro7 and transcription factors such as Val, Krx20 and Hoxb3, which are downstream of *vhnf1* and remain expressed in r5. According to this hypothesis, *iro7* represses *val* and *krx20* more efficiently than *vhnf1*. In addition, the initial positioning of this boundary is likely to depend mainly on *iro7*. Indeed, *iro7* expression is established before *vhnf1* expression reaches its definitive anterior limit, and therefore cannot depend totally on *vhnf1*. Consistently, in *vhnf1* mutants, the posterior expansion of *iro7* expression domain is limited to the length of one rhombomere. Other factors, such as retinoids, could be involved in positioning the *iro7* posterior boundary early on. According to this hypothesis, we observed a repression of *iro7* expression after treatment with retinoic acid (data not shown). Therefore, the main function of *vhnf1* repressive activity on *iro7* could be to refine the r4/r5 boundary.

iro7 is a divergent member of the Iro family, more closely related to the amniote *irx1/3* group of paralogues. *irx3* is expressed in the mouse neural plate during gastrulation (Bosse et al., 1997; Bellefroid et al., 1998). At the beginning of somitogenesis, the caudal limit of the *irx3* expression domain corresponds to the anterior limit of *vhnf1* expression and to the prospective r4/r5 boundary (S.S.M., V.L. and S. Cereghini, unpublished). Thus, mutual repression between Iro and vHnfl transcription factors and its involvement in the establishment of the r4/r5 boundary may constitute a conserved mechanism among vertebrates.

Setting up the r4 signalling centre

Establishing boundaries by mutual repression between two transcription factors expressed in adjacent territories is a common theme in early brain patterning. In several cases, these boundaries act as secondary signalling centres (Araki and Nakamura, 1999; Matsunaga et al., 2000; Kobayashi et al., 2002) (reviewed by Rhinn and Brand, 2001; Wurst and Bally-Cuif, 2001). Iroquois genes have been implicated in boundary formation both in *Drosophila* and vertebrates: in *Drosophila*, Iro genes act as dorsal selector genes in the eye/antenna imaginal disc and are involved in the formation of the DV organiser that prefigures the future equator in the adult eye (McNeill et al., 1997; Cavodeassi et al., 1999; Yang et al., 1999; Cavodeassi et al., 2000). In the chick forebrain, Irx3 is involved in the positioning of the zona limitans intrathalamica by mutual repression with Six3, another homeodomain transcription factor (Kobayashi et al., 2002). Our results show that *iro7*, despite its divergence, has a function similar to that of the other members of the family in positioning the r4/r5 boundary by mutual repression with another transcription factor.

Recent data suggest the presence of a novel signalling centre within the hindbrain, acting across the r4/r5 boundary (Maves et al., 2002; Walshe et al., 2002). In zebrafish embryos, *fgf3* and *fgf8* are both expressed early in r4 and are required for the expression of *krx20* and *val* in r5 and r5-r6, respectively (Maves et al., 2002; Walshe et al., 2002). Fgf3/8 signalling from r4 is also essential to the formation of the otic vesicle (Kwak et al., 2002; Leger and Brand, 2002; Maroon et al., 2002). The knockdown of *iro7* leads to a partial mis-specification of r4 but does not result in a reduction of *val* and *krx20* expression level. On the contrary, *val* expression domain in r5/r6 and *krx20* expression domain in r5 are expanded anteriorly. This shows that the r4 signalling centre is still functional, despite the reduction of r4 in *iro7* morphants. Examination of *fgf3* and *fgf8* expression in Moz7-injected embryos showed that the level of expression of these two genes in r4 is reduced, especially at early stages, but that their expression is not abolished. This result suggests that a reduced amount of Fgf3/8 signalling is sufficient to allow *val* and *krx20* expression. It is consistent with the data obtained previously (Wiellette and Sive, 2003), showing that *vhnf1* ectopic expression leads to ectopic activation of *val* and *krx20*, even though it represses *fgf8* expression in r4. Although FGF signalling in *iro7* morphants is sufficient to activate *val* and *krx20* expression, it may be too low for a correct specification of the otic vesicle, which is reduced and presents an abnormal rounded shape in Moz7-injected embryos.

What are the respective roles of *iro7* and the r4 signalling centre in setting up the r4/r5 boundary? FGFs and *iro7* have antagonistic functions on *val* and *krx20* activation. However, both signals act at different levels of the molecular hierarchy. FGFs are necessary to activate *val* and *krx20* expression in the *vhnf1* expressing territory, and are not involved in *vhnf1* activation. *iro7* is involved in repressing *val* and *krx20* expression but, at least in part, as a consequence of *vhnf1* repression. Thereby, *iro7* is involved in an earlier step that is the positioning of the boundary. Nothing is known about the molecular cues involved in *vhnf1* activation in the posterior neural plate. An interesting hypothesis would be that these cues are also present in future r4, and that *iro7* is required to repress the activation of *vhnf1* in this rhombomere.

A dual role for *iro7* in the anterior hindbrain

In this paper, we show that the anterior hindbrain is significantly reduced in the absence of Iro7. At the end of gastrulation, the anterior hindbrain markers *gbx1* (not shown) and *fgf8* are expressed both at a weaker level and in a reduced domain. Slightly later, the expression territories of *hoxa2* in r2-r3, *hoxb2* in r3-r4 (not shown) and *krx20* in r3 are also reduced, but none of them is totally absent. Therefore, the absence of *iro7* leads to an overall reduction of the anterior hindbrain but without any obvious mis-specification within this region.

We also demonstrate here that the knockdown of *iro7* leads to a strong reduction in the *ngn1*-expressing proneural clusters in the anterior hindbrain, especially in r4, whereas the more caudal proneural clusters are not affected. Moreover, *iro7* knockdown affects specific primary neuronal populations. The nuclei of the facial (VIIth) nerve and, to lesser extent of the trigeminal (Vth) nerve, are reduced, while the r4-derived Mauthner cells are always lost and the r2-derived RoL2 are also occasionally absent. Thus, in the absence of the Iro7 protein, neurogenesis is affected in the rostral hindbrain. Accordingly, *iro7* was previously shown to be necessary for the formation of the trigeminal ganglia (Itoh et al., 2002).

The defects we observed in the differentiation of some neuronal subtypes could result from a change in AP specification or from a direct effect of *iro7* on neurogenesis. We favour the second hypothesis for several reasons. First, the absence of r4 proneural clusters and of Mauthner neurons is unlikely to result only from the reduction of r4. Mauthner cells are indeed lost in 100% of the Moz7-injected embryos, although the transformation of r4 into r5 is never total and its extent is slightly variable from one embryo to the other. Second, we also observed a reduction of *ngn1* expression in r2 clusters, as well as an occasional loss of r2-derived RS neurons. As we mentioned above, the *iro7* knock-down leads to a reduction in size but not to a misspecification of the anterior hindbrain, so the neuronal defects in this region are likely to be linked to a role of *iro7* in neurogenesis. Third, no ectopic r5-specific RS neurons were observed, a phenotype that would be expected if the loss of Mauthner cells was due to a pure change in AP identity. Finally, ectopic expression of *iro7* activates *ngn1* and, in the neurectoderm, this activation has been proposed to result from a function of Iro7 as a transcriptional activator (Itoh et al., 2002). Thus, the activation of *ngn1* expression by Iro7 may be direct.

In conclusion, we propose that *iro7* has a dual function in the hindbrain: it is required for the positioning of the r4/r5 boundary by repressing *vhnf1*, and for neurogenesis in the anterior hindbrain, possibly by direct activation of *ngn1* expression. This dual function is consistent with the successive roles found for Iro genes in the *Drosophila* wing imaginal disc (Gomez-Skarmeta et al., 1996; Leyns et al., 1996; Grillenzoni et al., 1998; Diez del Corral et al., 1999; Calleja et al., 2002). Like its *Drosophila* cognate genes, *iro7* is required for successive steps of the patterning of an embryonic territory.

We are grateful to U. Strähle and P. Blader for providing us with the *pCS2-hGR* expression construct; to N. Hopkins and H. Okamoto for the gift of the *vhnf1*^{hi2169} and Isl11-GFP fish lines, respectively; to A. Chitnis for the gift of the *ngn1* probe and the Δ*N-iro7* construct; to V. Prince for the gift of the Hox probes; and to B. Thisse and C. Thisse for providing us with the *six3* and *vhnf1* probes, and the full-length *iro7*. We thank F. Bouallague for fish care; S. Cereghini, M. Itoh and A. Chitnis for fruitful discussions and for sharing unpublished material and data; L. Bally-Cuif for fruitful discussions and warm support; and P. Charnay, C. Vesque, S. Cereghini and J. Ghislain for critical reading of the manuscript. This work was supported by funds from the INSERM, FRM, ARC and MENRT. V.L. was supported by a fellowship from MENRT.

References

Araki, I. and Nakamura, H. (1999). Engrailed defines the position of dorsal di-mesencephalic boundary by repressing diencephalic fate. *Development* **126**, 5127-5135.

Bell, E., Wingate, R. J. and Lumsden, A. (1999). Homeotic transformation of rhombomere identity after localized Hoxb1 misexpression. *Science* **284**, 2168-2171.

Bellefroid, E. J., Kobbe, A., Gruss, P., Pieler, T., Gurdon, J. B. and Papalopulu, N. (1998). Xiro3 encodes a Xenopus homolog of the Drosophila Iroquois genes and functions in neural specification. *EMBO J.* **17**, 191-203.

Bosse, A., Zulch, A., Becker, M. B., Torres, M., Gomez-Skarmeta, J. L., Modolell, J. and Gruss, P. (1997). Identification of the vertebrate Iroquois

homeobox gene family with overlapping expression during early development of the nervous system. *Mech. Dev.* **69**, 169-181.
Burglin, T. R. (1997). Analysis of TALE superclass homeobox genes (MEIS, PBC, KNOX, Iroquois, TGIF) reveals a novel domain conserved between plants and animals. *Nucleic Acids Res.* **25**, 4173-4180.
Calleja, M., Renaud, O., Usui, K., Pistillo, D., Morata, G. and Simpson, P. (2002). How to pattern an epithelium: lessons from achaete-scute regulation on the notum of Drosophila. *Gene* **292**, 1-12.
Cavodeassi, F., Diez del Corral, R., Campuzano, S. and Dominguez, M. (1999). Compartments and organising boundaries in the Drosophila eye: the role of the homeodomain Iroquois proteins. *Development* **126**, 4933-4942.
Cavodeassi, F., Modolell, J. and Campuzano, S. (2000). The Iroquois homeobox genes function as dorsal selectors in the Drosophila head. *Development* **127**, 1921-1929.
Cavodeassi, F., Modolell, J. and Gomez-Skarmeta, J. L. (2001). The Iroquois family of genes: from body building to neural patterning. *Development* **128**, 2847-2855.
Chandrasekhar, A., Moens, C. B., Warren, J. T., Jr, Kimmel, C. B. and Kuwada, J. Y. (1997). Development of branchiomotor neurons in zebrafish. *Development* **124**, 2633-2644.
Choe, S. K., Vlachakis, N. and Sagerstrom, C. G. (2002). Meis family proteins are required for hindbrain development in the zebrafish. *Development* **129**, 585-595.
Cordes, S. P. and Barsh, G. S. (1994). The mouse segmentation gene kr encodes a novel basic domain-leucine zipper transcription factor. *Cell* **79**, 1025-1034.
Diez del Corral, R., Aroca, P., Gomez-Skarmeta, J. L., Cavodeassi, F. and Modolell, J. (1999). The Iroquois homeodomain proteins are required to specify body wall identity in Drosophila. *Genes Dev.* **13**, 1754-1761.
Ericson, J., Thor, S., Edlund, T., Jessell, T. M. and Yamada, T. (1992). Early stages of motor neuron differentiation revealed by expression of homeobox gene Islet-1. *Science* **256**, 1555-1560.
Ferretti, E., Marshall, H., Popperl, H., Maconochie, M., Krumlauf, R. and Blasi, F. (2000). Segmental expression of Hoxb2 in r4 requires two separate sites that integrate cooperative interactions between Prep1, Pbx and Hox proteins. *Development* **127**, 155-166.
Furley, A. J., Morton, S. B., Manalo, D., Karagogeos, D., Dodd, J. and Jessell, T. M. (1990). The axonal glycoprotein TAG-1 is an immunoglobulin superfamily member with neurite outgrowth-promoting activity. *Cell* **61**, 157-170.
Furthauer, M., Thisse, C. and Thisse, B. (1997). A role for FGF-8 in the dorsoventral patterning of the zebrafish gastrula. *Development* **124**, 4253-4264.
Giudicelli, F., Taillebourg, E., Charnay, P. and Gilardi-Hebenstreit, P. (2001). *Krox-20* patterns the hindbrain through both cell-autonomous and non cell-autonomous mechanisms. *Genes Dev.* **15**, 567-580.
Giudicelli, F., Gilardi-Hebenstreit, P., Mechta-Grigoriou, F., Poquet, C. and Charnay, P. (2003). Novel activities of Mafb underlie its dual role in hindbrain segmentation and regional specification. *Dev. Biol.* **253**, 150-162.
Gomez-Skarmeta, J. L., del Corral, R. D., de la Calle-Mustienes, E., Ferre-Marco, D. and Modolell, J. (1996). Araucan and caupolican, two members of the novel iroquois complex, encode homeoproteins that control proneural and vein-forming genes. *Cell* **85**, 95-105.
Gomez-Skarmeta, J. L., Glavic, A., de la Calle-Mustienes, E., Modolell, J. and Mayor, R. (1998). Xiro, a Xenopus homolog of the Drosophila Iroquois complex genes, controls development at the neural plate. *EMBO J.* **17**, 181-190.
Gomez-Skarmeta, J. L. and Modolell, J. (2002). Iroquois genes: genomic organization and function in vertebrate neural development. *Curr. Opin. Genet. Dev.* **12**, 403-408.
Graham, A. and Lumsden, A. (1996). Interactions between rhombomeres modulate Krox-20 and follistatin expression in the chick embryo hindbrain. *Development* **122**, 473-480.
Grillenzoni, N., van Helden, J., Dambly-Chaudiere, C. and Ghysen, A. (1998). The iroquois complex controls the somatotopy of Drosophila notum mechanosensory projections. *Development* **125**, 3563-3569.
Guthrie, S. and Lumsden, A. (1991). Formation and regeneration of rhombomere boundaries in the developing chick hindbrain. *Development* **112**, 221-229.
Guthrie, S., Prince, V. and Lumsden, A. (1993). Selective dispersal of avian rhombomere cells in orthotopic and heterotopic grafts. *Development* **118**, 527-538.
Hanneman, E., Trevarrow, B., Metcalfe, W. K., Kimmel, C. B. and Westerfield, M. (1988). Segmental pattern of development of the hindbrain and spinal cord of the zebrafish embryo. *Development* **103**, 49-58.
Hatta, K. (1992). Role of the floor plate in axonal patterning in the zebrafish CNS. *Neuron* **9**, 629-642.
Hauptmann, G. and Gerster, T. (1994). Two-color whole-mount in situ hybridization to vertebrate and Drosophila embryos. *Trends Genet.* **10**, 266.
Helmbacher, F., Pujades, C., Desmarquet, C., Frain, M., Rijli, F. M., Chambon, P. and Charnay, P. (1998). Hoxa1 and Krox-20 synergize to control the development of rhombomere 3. *Development* **125**, 4739-4748.
Higashijima, S., Hotta, Y. and Okamoto, H. (2000). Visualization of cranial motor neurons in live transgenic zebrafish expressing green fluorescent protein under the control of the islet-1 promoter/enhancer. *J. Neurosci.* **20**, 206-218.
Irving, C., Nieto, M. A., DasGupta, R., Charnay, P. and Wilkinson, D. G. (1996). Progressive spatial restriction of Sek-1 and Krox-20 gene expression during hindbrain segmentation. *Dev. Biol.* **173**, 26-38.
Itoh, M., Kudoh, T., Dedekian, M., Kim, C. H. and Chitnis, A. B. (2002). A role for iro1 and iro7 in the establishment of an anteroposterior compartment of the ectoderm adjacent to the midbrain-hindbrain boundary. *Development* **129**, 2317-2327.
Jungbluth, S., Bell, E. and Lumsden, A. (1999). Specification of distinct motor neuron identities by the singular activities of individual Hox genes. *Development* **126**, 2751-2758.
Kimmel, C. B., Ballard, W. W., Kimmel, S. R., Ullmann, B. and Schilling, T. F. (1995). Stages of embryonic development of the zebrafish. *Dev. Dyn.* **203**, 253-310.
Kobayashi, D., Kobayashi, M., Matsumoto, K., Ogura, T., Nakafuku, M. and Shimamura, K. (2002). Early subdivisions in the neural plate define distinct competence for inductive signals. *Development* **129**, 83-93.
Krauss, S., Johansen, T., Korzh, V. and Fjose, A. (1991). Expression of the zebrafish paired box gene pax[zf-b] during early neurogenesis. *Development* **113**, 1193-1206.
Krauss, S., Maden, M., Holder, N. and Wilson, S. W. (1992). Zebrafish pax[b] is involved in the formation of the midbrain-hindbrain boundary. *Nature* **360**, 87-89.
Kudoh, T., Tsang, M., Hukriede, N. A., Chen, X., Dedekian, M., Clarke, C. J., Kiang, A., Schultz, S., Epstein, J. A., Toyama, R. et al. (2001). A gene expression screen in zebrafish embryogenesis. *Genome Res.* **11**, 1979-1987.
Kwak, S. J., Phillips, B. T., Heck, R. and Riley, B. B. (2002). An expanded domain of fgf3 expression in the hindbrain of zebrafish valentino mutants results in mis-patterning of the otic vesicle. *Development* **129**, 5279-5287.
Larsen, C. W., Zeltser, L. M. and Lumsden, A. (2001). Boundary formation and compartition in the avian diencephalon. *J. Neurosci.* **21**, 4699-4711.
Lecaudey, V., Thisse, C., Thisse, B. and Schneider-Maunoury, S. (2001). Sequence and expression pattern of ziro7, a novel, divergent zebrafish iroquois homeobox gene. *Mech. Dev.* **109**, 383-388.
Leger, S. and Brand, M. (2002). Fgf8 and Fgf3 are required for zebrafish ear placode induction, maintenance and inner ear patterning. *Mech. Dev.* **119**, 91-108.
Leyns, L., Gomez-Skarmeta, J. L. and Dambly-Chaudiere, C. (1996). iroquois: a prepattern gene that controls the formation of bristles on the thorax of Drosophila. *Mech. Dev.* **59**, 63-72.
Lumsden, A. and Krumlauf, R. (1996). Patterning the vertebrate neuraxis. *Science* **274**, 1109-1115.
Marin, F. and Charnay, P. (2000). Hindbrain patterning: FGFs regulate Krox20 and mafB/kr expression in the otic/preotic region. *Development* **127**, 4925-4935.
Maroon, H., Walshe, J., Mahmood, R., Kiefer, P., Dickson, C. and Mason, I. (2002). Fgf3 and Fgf8 are required together for formation of the otic placode and vesicle. *Development* **129**, 2099-2108.
Matsunaga, E., Araki, I. and Nakamura, H. (2000). Pax6 defines the di-mesencephalic boundary by repressing En1 and Pax2. *Development* **127**, 2357-2365.
Maves, L., Jackman, W. and Kimmel, C. B. (2002). FGF3 and FGF8 mediate a rhombomere 4 signaling activity in the zebrafish hindbrain. *Development* **129**, 3825-3837.
McClintock, J. M., Carlson, R., Mann, D. M. and Prince, V. E. (2001). Consequences of Hox gene duplication in the vertebrates: an investigation of the zebrafish Hox paralogue group 1 genes. *Development* **128**, 2471-2484.
McClintock, J. M., Kheirbek, M. A. and Prince, V. E. (2002). Knockdown of duplicated zebrafish hoxb1 genes reveals distinct roles in hindbrain patterning and a novel mechanism of duplicate gene retention. *Development* **129**, 2339-2354.
McNeill, H., Yang, C. H., Brodsky, M., Ungos, J. and Simon, M. A. (1997).

mirror encodes a novel PBX-class homeoprotein that functions in the definition of the dorsal-ventral border in the Drosophila eye. *Genes Dev.* **11**, 1073-1082.

Metcalfe, W. K., Mendelson, B. and Kimmel, C. B. (1986). Segmental homologies among reticulospinal neurons in the hindbrain of the zebrafish larva. *J. Comp. Neurol.* **251**, 147-159.

Moens, C. B., Cordes, S. P., Giorgianni, M. W., Barsh, G. S. and Kimmel, C. B. (1998). Equivalence in the genetic control of hindbrain segmentation in fish and mouse. *Development* **125**, 381-391.

Moens, C. B. and Prince, V. E. (2002). Constructing the hindbrain: Insights from the zebrafish. *Dev. Dyn.* **224**, 1-17.

Morrison, A. D. (1998). 1 + 1=r4 and much much more. *BioEssays* **20**, 794-797.

Murphy, P. and Hill, R. E. (1991). Expression of the mouse labial-like homeobox-containing genes, Hox 2.9 and Hox 1.6, during segmentation of the hindbrain. *Development* **111**, 61-74.

Nasevicius, A. and Ekker, S. C. (2000). Effective targeted gene 'knockdown' in zebrafish. *Nat. Genet.* **26**, 216-220.

Oxtoby, E. and Jowett, T. (1993). Cloning of the zebrafish krox-20 gene (krx-20) and its expression during hindbrain development. *Nucleic Acids Res.* **21**, 1087-1095.

Popperl, H., Rikhof, H., Chang, H., Haffter, P., Kimmel, C. B. and Moens, C. B. (2000). lazarus is a novel pbx gene that globally mediates hox gene function in zebrafish. *Mol. Cell* **6**, 255-267.

Prince, V. E., Moens, C. B., Kimmel, C. B. and Ho, R. K. (1998). Zebrafish hox genes: expression in the hindbrain region of wild-type and mutants of the segmentation gene, valentino. *Development* **125**, 393-406.

Rhinn, M. and Brand, M. (2001). The midbrain–hindbrain boundary organizer. *Curr. Opin. Neurobiol.* **11**, 34-42.

Rijli, F. M., Gavalas, A. and Chambon, P. (1998). Segmentation and specification in the branchial region of the head: the role of the Hox selector genes. *Int. J. Dev. Biol.* **42**, 393-401.

Rupp, R. A., Snider, L. and Weintraub, H. (1994). Xenopus embryos regulate the nuclear localization of XMyoD. *Genes Dev.* **8**, 1311-1323.

Schneider-Maunoury, S., Gilardi-Hebenstreit, P. and Charnay, P. (1998). How to build a vertebrate hindbrain. Lessons from genetics. *C. R. Acad. Sci. Iii* **321**, 819-834.

Sun, Z. and Hopkins, N. (2001). vhnf1, the MODY5 and familial GCKD-associated gene, regulates regional specification of the zebrafish gut, pronephros, and hindbrain. *Genes Dev.* **15**, 3217-3229.

Torres, M. and Giraldez, F. (1998). The development of the vertebrate inner ear. *Mech. Dev.* **71**, 5-21.

Trainor, P. A. and Krumlauf, R. (2000). Patterning the cranial neural crest: hindbrain segmentation and Hox gene plasticity. *Nat. Rev. Neurosci.* **1**, 116-124.

Voiculescu, O., Taillebourg, E., Pujades, C., Kress, C., Buart, S., Charnay, P. and Schneider-Maunoury, S. (2001). Hindbrain patterning: Krox20 couples segmentation and specification of regional identity. *Development* **128**, 4967-4978.

Walshe, J., Maroon, H., McGonnell, I. M., Dickson, C. and Mason, I. (2002). Establishment of Hindbrain Segmental Identity Requires Signaling by FGF3 and FGF8. *Curr. Biol.* **12**, 1117-1123.

Westerfield, M. (1994). *The Zebrafish Book*, 2.1 edn. Eugene, OR: University of Oregon Press.

Wiellette, E. L. and Sive, H. (2003). vhnf1 and Fgf signals synergize to specify rhombomere identity in the zebrafish hindbrain. *Development* **130**, 3821-3829.

Wilkinson, D. G., Bhatt, S., Chavrier, P., Bravo, R. and Charnay, P. (1989). Segment-specific expression of a zinc-finger gene in the developing nervous system of the mouse. *Nature* **337**, 461-464.

Wizenmann, A. and Lumsden, A. (1997). Segregation of rhombomeres by differential chemoaffinity. *Mol. Cell Neurosci.* **9**, 448-459.

Wurst, W. and Bally-Cuif, L. (2001). Neural plate patterning: upstream and downstream of the isthmic organizer. *Nat. Rev. Neurosci.* **2**, 99-108.

Xu, Q., Alldus, G., Holder, N. and Wilkinson, D. G. (1995). Expression of truncated Sek-1 receptor tyrosine kinase disrupts the segmental restriction of gene expression in the Xenopus and zebrafish hindbrain. *Development* **121**, 4005-4016.

Xu, Q., Mellitzer, G., Robinson, V. and Wilkinson, D. G. (1999). In vivo cell sorting in complementary segmental domains mediated by Eph receptors and ephrins. *Nature* **399**, 267-271.

Yang, C. H., Simon, M. A. and McNeill, H. (1999). mirror controls planar polarity and equator formation through repression of fringe expression and through control of cell affinities. *Development* **126**, 5857-5866.